

ACOUSTIC WAVE PROPAGATION IN HIGH SCALE IMPEDANCE MISMATCH MEDIUMS

**MD RABIUL AWAL^{1*}, MUZAMMIL JUSOH², MUHAMMAD SYARIFUDDIN YAHYA¹,
NURUL ADILAH ABDUL LATIFF¹, SALISA ABDUL RAHMAN¹, AHMAD NAZRI
DAGANG¹, HIDAYATUL AINI ZAKARIA¹ AND SHAKIR SAAT³**

¹*Faculty of Ocean Engineering, Technology and Informatics, Universiti Malaysia Terengganu,
21030 Kuala Nerus, Terengganu, Malaysia*

²*BioEM, School of Computer and Communication Engineering, Universiti Malaysia Perlis
(UniMAP), Kampus Pauh Putra, 02600 Arau, Perlis, Malaysia*

³*School of Computing and Informatics, Albukhary International University,
Jalan Langgar, Alor Setar Kedah, Malaysia*

*Corresponding author: rabiulawal1@gmail.com

(Received: 29th July 2020; Accepted: 20th February 2021; Published on-line: 4th July 2021)

ABSTRACT: A finite element analysis of acoustic propagation in a multilayered medium is presented in this paper. A circular transmitter (diameter 14 mm, thickness 3 mm) and a rectangular receiver ($20 \times 10 \times 0.5$ mm³) are set to detect the variations in the propagation pattern. A complex medium ($70 \times 40 \times 60$ mm³) composed of skin, fat, muscle, bone and liquid is designed in a simulated environment. A scale of frequencies (10 kHz to 2 MHz) is applied to trace the impact on the propagation pattern as well. It is found from the analysis that fat and liquid layers affect the acoustic propagation the most (-69 dB), which results in a significant drop in the received sound pressure level at the receiving end. Again, other than skin and fat layers, low frequencies (less than 1 MHz) are more beneficial in terms of sound pressure level. However, higher frequencies contribute to lower displacements at the receiving end, which will cause less power potential as well.

ABSTRAK: Analisis elemen terhingga bagi penyebaran akustik dalam medium berlapis dibentangkan dalam kajian ini. Pemancar bulat (diameter 14 mm, ketebalan 3 mm) dan penerima segi empat tepat ($20 \times 10 \times 0.5$ mm³) diatur bagi mengesan perubahan pola penyebaran. Medium kompleks ($70 \times 40 \times 60$ mm³) yang terdiri daripada kulit, lemak, otot, tulang dan cecair direka dalam persekitaran simulasi. Skala frekuensi (10 kHz hingga 2 MHz) digunakan bagi mengesan corak penyebaran. Dapatkan kajian menunjukkan bahawa lapisan lemak dan cecair mempengaruhi penyebaran akustik (-69 dB), yang mengakibatkan penurunan mendadak tahap penerimaan tekanan bunyi di hujung penerima. Selain lapisan kulit dan lemak, frekuensi rendah (kurang dari 1 MHz) adalah lebih berguna dari segi tahap tekanan suara. Walau bagaimanapun, frekuensi lebih tinggi menyebabkan kurang anjakan di hujung penerima, sekaligus mengurangkan potensi daya tenaga.

KEYWORDS: acoustic energy transfer; acoustic wave; ZnO, multilayered medium; impedance mismatch

1. INTRODUCTION

Wireless power transfer (WPT) has drawn significant industrial attention in recent times. The initial intention of this scientific module was to provide mobility to handheld devices. Soon, it was realized that over kW range power can be transferred wirelessly by

WPT. To do so, inductive, capacitive, microwave, and acoustic coupling can be used. Among these, inductive WPT is widely practiced and commercially available with high efficiency and power (30 kW) [1-3]. It was recently reported that 5 to 7 meter separation distance between receiver and transmitter was achieved by inductive WPT [4, 5]. Nevertheless, inductive WPT suffers from coupling misalignment and penetration losses [6]. Capacitive WPT is still in the developing stage. Unfortunately, the inverse property of capacitance to distance limits the separation (<1 mm) and efficiency of this WPT [7-10]. Microwave WPT can provide very high efficiency and wide propagation area as well, due to its high energy density penetration [11-13]. Again, optical WPT is capable of transmitting energy over a long range (>km), however, suffers from the requirement for a line of sight [14-16].

Acoustic energy transfer (AET), unlike the aforementioned WPTs, transfers power by propagating energy as sound or vibration waves [17]. The propagated energy is then collected by a receiver which converts the vibration energy to useful electrical energy. To do so, piezoelectric conversion termed as piezoelectricity is practiced so far. Recent interest in wireless powering of implantable devices added to the need to study acoustic propagation in a complex multilayered medium with high scale impedance mismatch, which closely characterizes the human body. Hence, in this paper, we have designed a multilayer medium that is composed of the same type of layers available in the human body. We have considered a wireless pacemaker system and hence, we have limited our study to the human chest only.

The scope of this paper includes a finite element analysis of the acoustic wave propagation in a multilayered medium. The medium is specific for very high impedance mismatched layers. As we are considering AET for implants, it is worthy to investigate the impact of the medium with different physical characteristics. Also, the effect of applying a wide range of frequencies (10 kHz to 2 MHz) is considered in the scope. Nevertheless, dynamic receivers or transmitters are not considered in this study, rather we have considered the fixed locations for the transmitter and receiver.

2. MODELLING IN FINITE ELEMENT ANALYSIS

It is possible to analyze the acoustic propagation under a simulated environment using finite elements. Hence, the system is designed and analyzed with finite elements. As such, a transmitter-receiver coupling is designed for the finite element analysis. The transmitter is a simple circular transceiver with a zinc oxide (ZnO) layer and an aluminum (Al) layer. It is 14 mm in diameter and 3 mm in thickness (Al layer 1 mm and ZnO 2 mm). In contrast, the receiver is a simple ZnO rectangular block with a $20 \times 10 \times 0.5$ mm³ dimension. The reason to keep the transmitter in circular shape is to use the benefit of the directional acoustic beams. Also, a rectangular configuration is more beneficial as receiver [18]. The transmitter and receiver are depicted in Fig. 1.

The medium is designed to resemble human chest layers. It is a $70 \times 40 \times 60$ mm³ block with skin, fat, muscle, bone and liquid (water) layers. Hence, the medium reflects a very high scale impedance mismatch within the layers. An additional liquid block is added to compensate for the medium impedance. The medium details are given in Fig. 2 and Table 1.

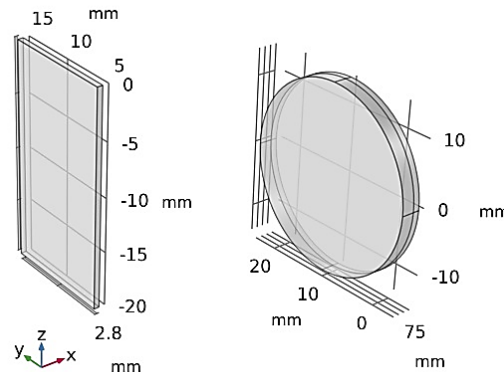


Fig. 1: Transmitter and receiver.

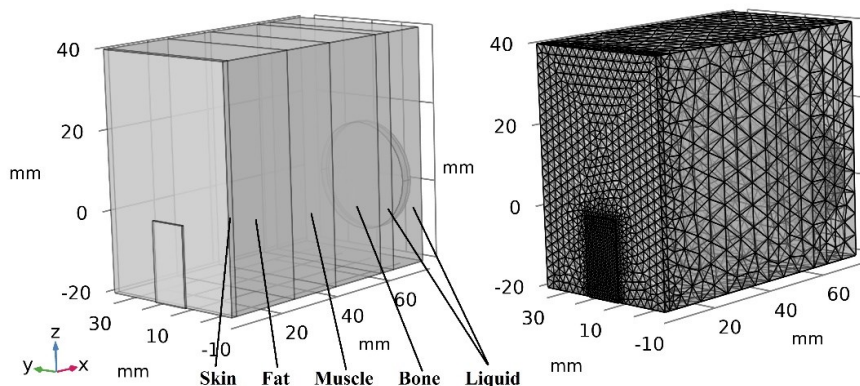


Fig. 2: Propagation medium model and mesh.

Table 1: Human chest as medium

Medium	Dimension [mm ³]	Density[kg/m ³]
Medium	70×40×60	
Skin	1.5×40×60	1109
Fat	20×40×60	911
Muscle	15×40×60	1090
Bone	17×40×60	1908
Liquid 1	5×40×60	997
Liquid 2	11.5×40×60	997

Table 2: SPL in the medium layers

Medium	Max SPL [dB]	Min SPL [dB]
Skin	129	82
Fat	129	74
Muscle	129	70
Bone	130	52
Liquid 1	126	57
Liquid 2	132	68

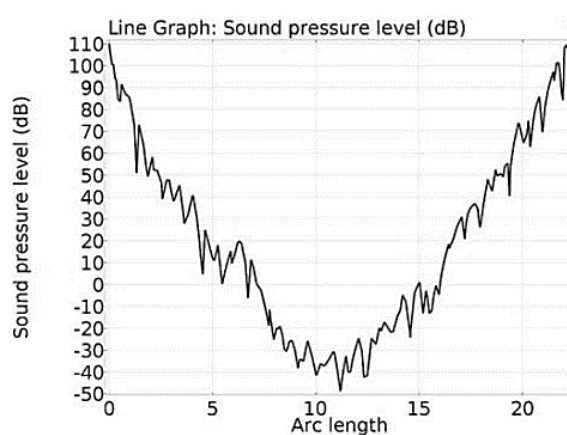


Fig. 3: Sound pressure level received by the PZT receiver.

3. ACOUSTIC PROFILE AND ANALYSIS

Figures 3, 4, and 5 describe the propagation pattern and received sound pressure level by the rectangular receiver. From the figures, it is clear that fat and liquid layers contribute to decreasing the acoustic pressure field and sound pressure level. However, the irregular spatial acoustic beam formation is observed as well. The sound striking the receiving cantilever does so with a pressure value of approximately 111 dB to as high as 114 dB. A more focused presentation of the received sound pressure level is placed in Fig. 5. The electric potential generated in the receiver terminal has the range of $-9.0320\text{e-}15$ to $-5.6501\text{e-}13$ volt. The total displacement in the receiver is found to be $6.94\text{e-}9$ mm. Again, the maximum stress on the receiver is 31.4 Pa.

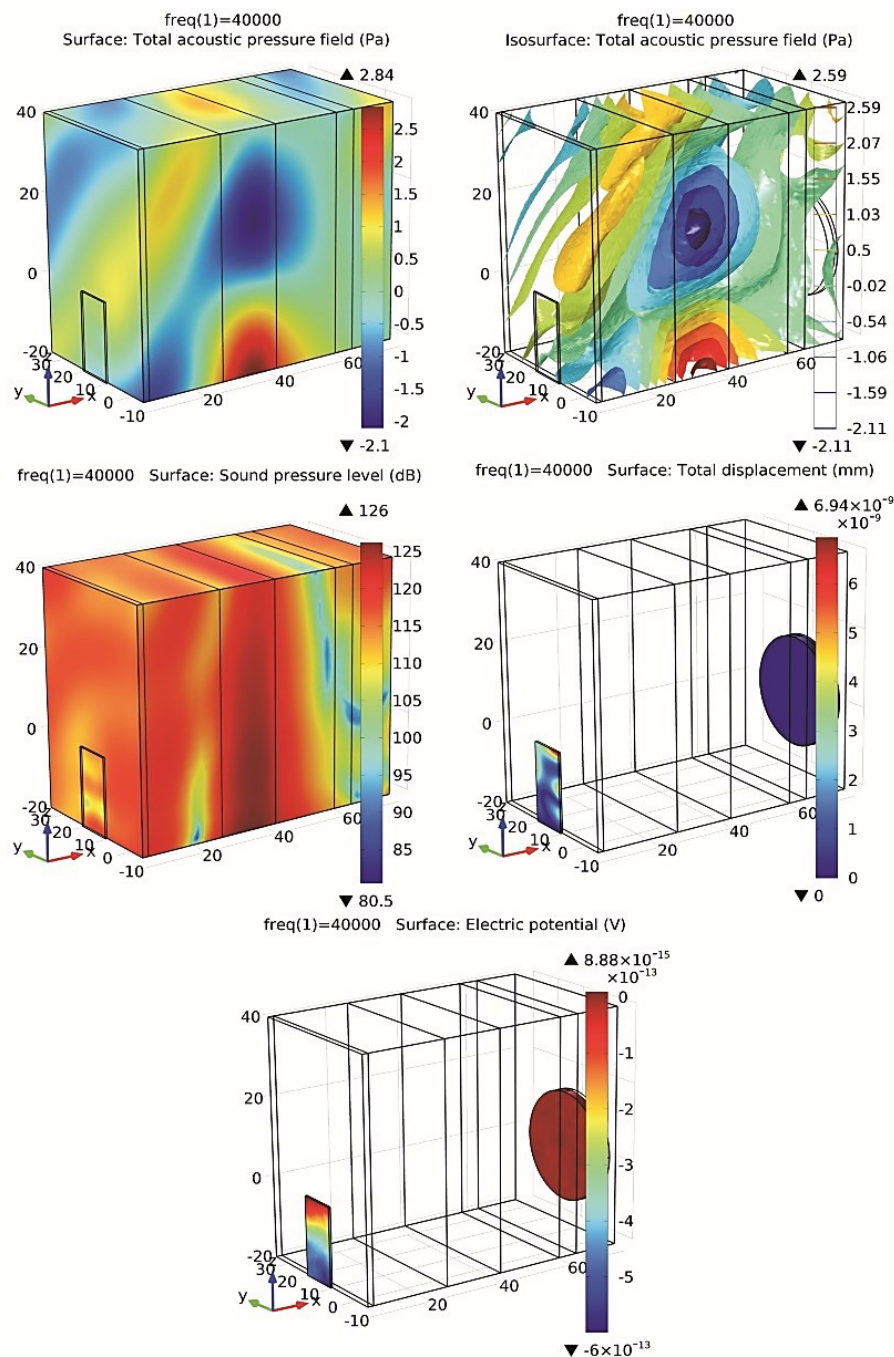


Fig. 4: Acoustic propagation within the layered medium (sample data at 40 kHz).

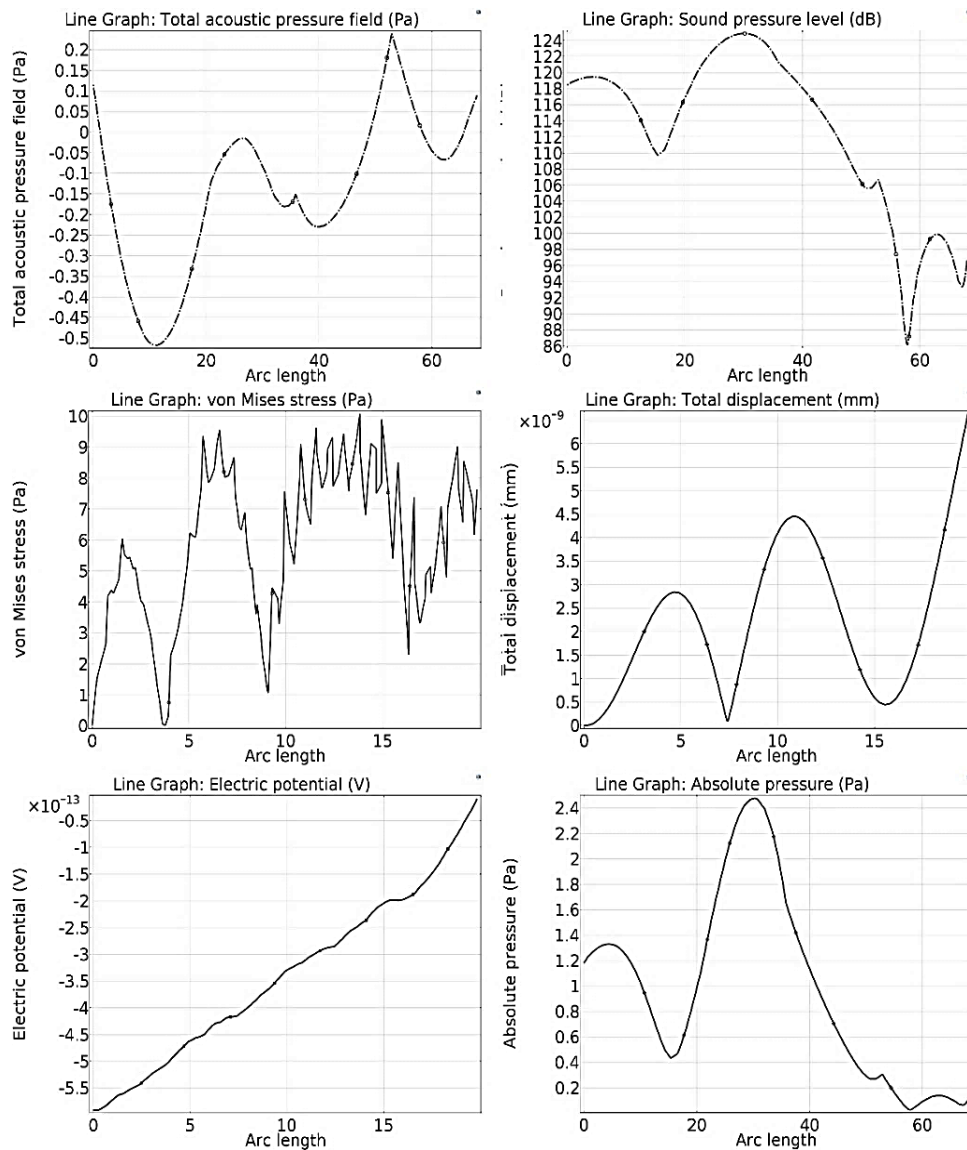


Fig. 5: Descriptions of the wave parameters (sample data at 40 kHz).

Figures 4 and 5 depict wave parameters of the transmitted acoustic waves on the attached wall with the receiver (which has a height of 60 mm) of the considered medium. The impacts of an applied frequency of 40 kHz is presented here. The results suggest that low-density mediums mostly impact the acoustic pressure fields. These result in weaker SPL to the next medium. However, if we increase the applied frequency, the reflections within the medium become more severe. In fact, at 2 MHz, the self-reflection becomes visible and mainly located between the two liquid layers. Figure 3 presents the SPL reflected by the receiver. It is clear from the figure that the reflected SPL can vary from 110 to -50 dB. Also, the reflections mainly occurred in the middle of the receiver even though it is placed at the bottom end of the medium.

Figure 6 presents the SPL against the applied frequencies on the layer with the attached receiver. The applied frequency range is 10 kHz to 2 MHz. The SPL varied from as low as 68 dB to as high as 132 dB. The lowest SPL is found at 1.45 MHz (68 dB) whereas the highest SPL values are available close to 1.21 MHz (132 dB). Hence, it is clear from the figure that the SPL distribution is not benefitted by the frequency increment.

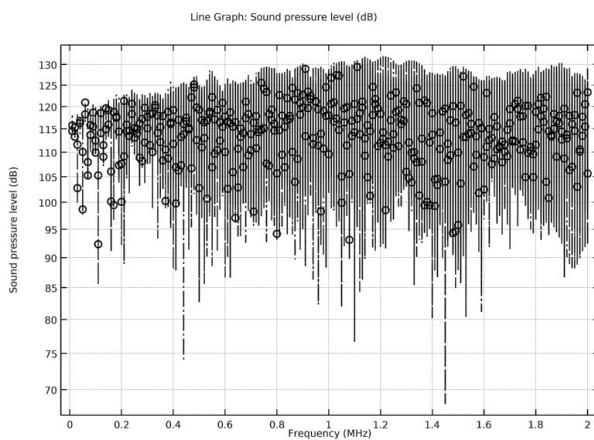


Fig. 6: SPL versus frequency plot.

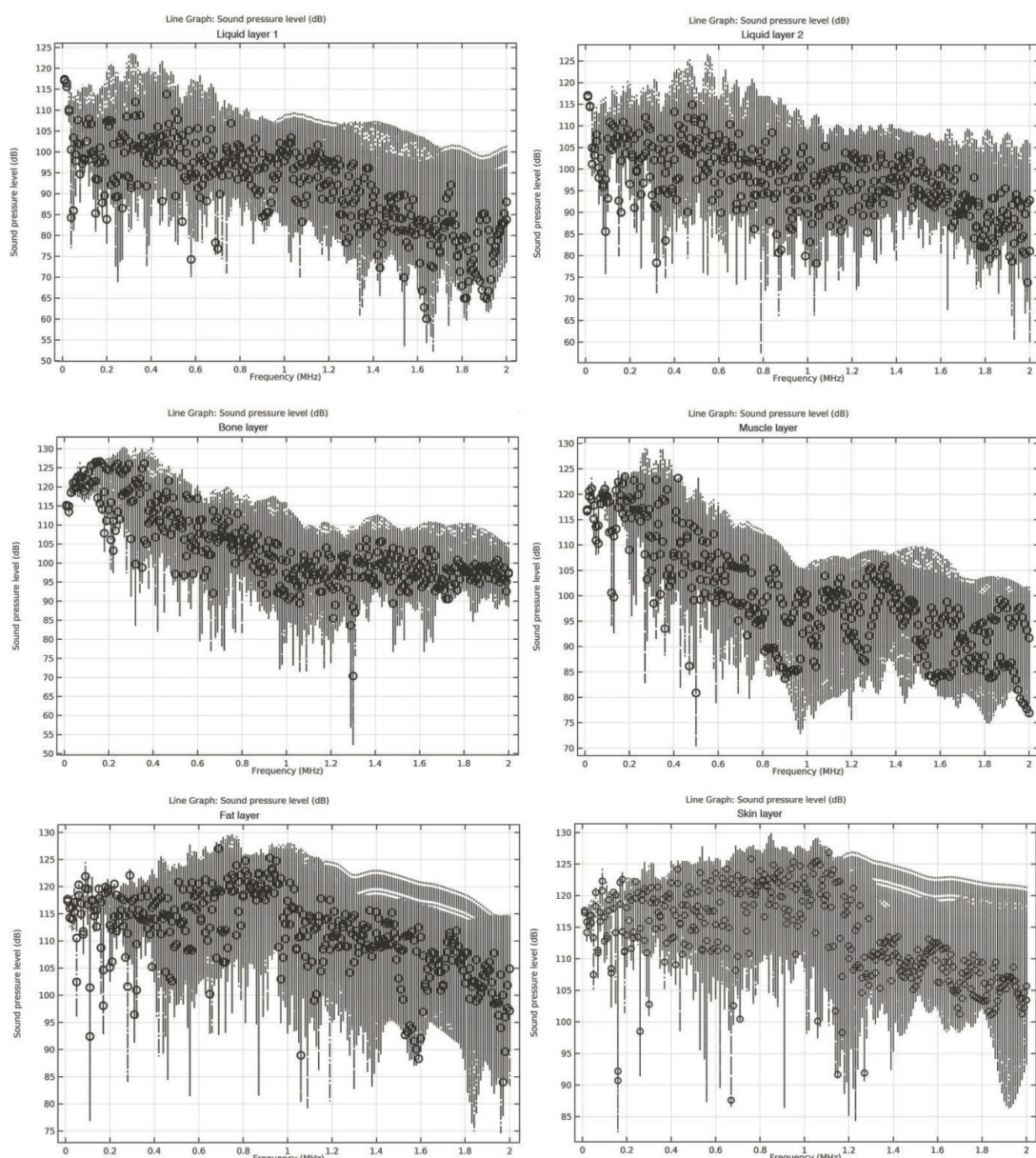


Fig. 7: SPL variations in different layers of the medium (applied frequency range 10 kHz – 2 MHz).

Figure 7 and Table 2 describe the more specified SPL profile according to the layers of the medium. According to the design, there are six layers in total between the transmitter and the receiver. Layer 1 and layer 2 are of liquid material. In layer 1, min observed SPL is approximately 68 dB at 1.45 MHz, whereas, max SPL is 132 dB at 1.21 MHz. In layer 2, min SPL drops down to approximately 57 dB at 0.79 MHz, and max SPL to 126 dB at 0.55 MHz. The SPL drops even more in layer 3 to min approximately 52 dB at 1.3 MHz whereas, max 130 dB is found at 0.27 and 0.35 MHz. Layer 4, 5, and 6 are of muscle, fat, and skin, respectively. For the muscle layer, min SPL received is approximately 70 dB at 0.5 MHz, and max is approximately 129 dB at 0.27 MHz.

Layer 5, which is the fat layer of 20 mm thickness, experiences min SPL of approximately 74 dB at 1.96 MHz, and max approximately 129 dB at 0.73, 0.74, and 0.75 MHz frequencies. Comparatively, in layer 6, the skin layer, min SPL is approximately 82 dB at 1.6 MHz, and max SPL is approximately 129 dB at 0.84, 0.85, 1.05 and 1.06 MHz frequencies.

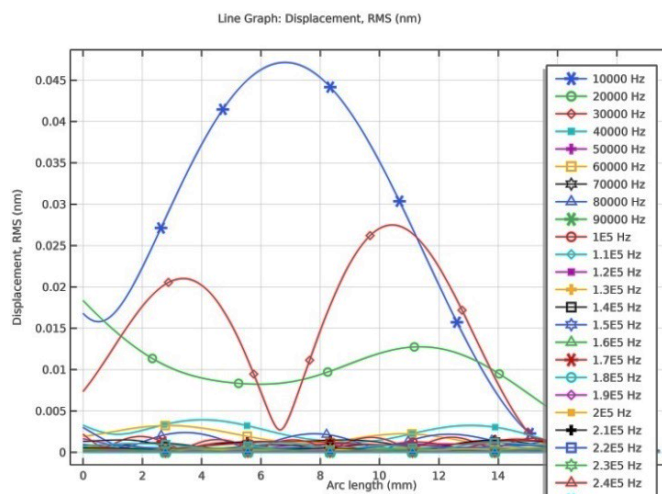


Fig. 8: Displacements occurred in the receiver (top blue, green and red are 10 kHz, 20 kHz and 30 kHz respectively).

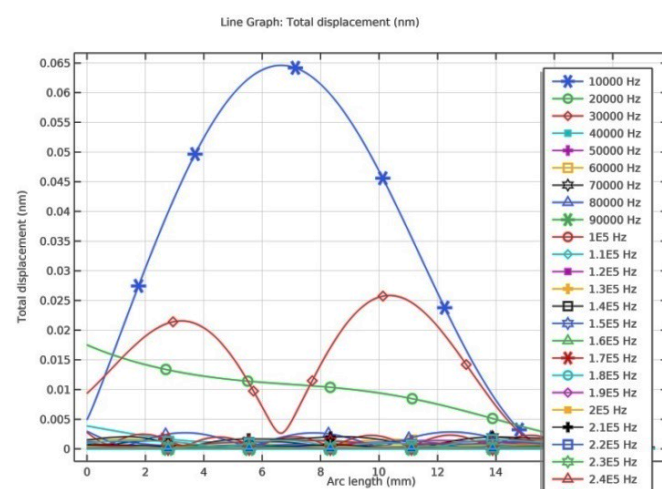


Fig. 9: Total displacements occurred in the receiver (top blue, green and red are 10 kHz, 20 kHz and 30 kHz respectively).

Figures 8 and 9 show the displacements that occurred in the receiver. Root mean square (RMS) of displacements is presented in Fig. 8 while the total displacements are shown in

Fig. 9. Interestingly, increased frequencies have decreased the displacements in the receiver. As the wavelength becomes smaller, it is losing power as well. From the figure we can see, 0.065 nm total displacements are observed (RMS 0.047 nm) for 10 kHz applied frequency. In comparison, 0.04 nm (RMS 0.028 nm) for 30 kHz, and less than 0.01 nm (RMS 0.047 nm) for 20 kHz. The rest of the frequencies will cause less than 0.004 nm displacements.

From the aforementioned results, it is noticeable that increasing frequencies is not going to be beneficial in the context of displacements that will directly impact the AET performance. For acoustic energy transfer, the transmitted energy will be collected by the receiver in the form of acoustic vibrations. Now, vibration will cause certain displacements in the receiver and the relationship is linear. Higher vibration will certainly cause higher displacements. In relation, higher displacements in piezoelectric layers will benefit with a higher electrical output which is the ultimate goal of a wireless power transfer system. Therefore, it is evident that for AET lower frequencies are preferable for implantable devices.

4. CONCLUSION

Finite element analysis of acoustic wave propagation in a very high scale impedance mismatch medium is presented in this paper. The analysis is mainly focused on acoustic energy transfer for implantable wireless devices as the medium contains a wide range of impedances. A circular transmitter and a rectangular receiver are paired to transfer acoustic waves in a multilayered medium that replicates the high scale impedance mismatch. A prescribed vibration is generated in the transmitter which is collected by the receiver to evaluate the impact of the multilayer configuration on the acoustic propagation. Sound pressure level (SPL) and receiver displacements are particularly focused to trace the effect of wide scale applied frequencies. It is found from the results that the SPL can be varied from as low as 68 dB (1.45 MHz) to as high as 132 dB (1.21 MHz). Hence, it is clear from the figure that the SPL distribution is not benefitted by the frequency increment. The electric potential generated in the receiver terminal has the range of -9.0320e-15 to -5.6501e-13 volts. The total displacement in the receiver is found to be 6.94e-9 mm. Again, the maximum stress on the receiver is 31.4 Pa. Therefore, as conclusion, the increased frequency can benefit the SPL while it decreases the displacements in the receiving end. As the displacement magnitude directly impacts the receiver performances, it is more beneficial to use less than MHz range frequencies for acoustic energy transfer applications.

ACKNOWLEDGEMENT

This work is partially supported by Universiti Malaysia Terengganu, under fundamental research grant scheme (Ref: FRGS/1/2019/TK04/UMT/03/1), Ministry of Higher Education, Government of Malaysia.

REFERENCES

- [1] Kurs A, Karalis A, Moffatt R, Joannopoulos JD, Fisher P, Soljačić M. (2007) Wireless power transfer via strongly coupled magnetic resonances. *Science*, 317(5834): 83-86. doi: 10.1126/science.114325
- [2] Wang CS, Covic GA, Stielau OH. (2004) Power transfer capability and bifurcation phenomena of loosely coupled inductive power transfer systems. *IEEE Transactions on Industrial Electronics*, 51(1): 148-157. doi: 10.1109/TIE.2003.822038.
- [3] Wang CS, Stielau OH, Covic GA. (2005) Design considerations for a contactless electric vehicle battery charger. *IEEE Transactions on Industrial Electronics*, 52(5): 1308-1314.

- doi: 10.1109/TIE.2005.855672.
- [4] Waffenschmidt E, Staring T. (2009) Limitation of inductive power transfer for consumer applications. In 2009 13th European Conference on Power Electronics and Applications (pp. 1-10). IEEE.
- [5] Park C, Lee S, Cho GH, Rim CT. (2014) Innovative 5-m-off-distance inductive power transfer systems with optimally shaped dipole coils. *IEEE Transactions on Power Electronics*, 30(2): 817-827. doi: 10.1109/TPEL.2014.2310232.
- [6] Choi, BH, Lee ES, Kim JH, Rim CT. (2014) 7m-off-long-distance extremely loosely coupled inductive power transfer systems using dipole coils. In 2014 IEEE Energy Conversion Congress and Exposition (ECCE) (pp. 858-863). IEEE.
- [7] Kim A, Ochoa M, Rahimi R, Ziaie B. (2015) New and emerging energy sources for implantable wireless microdevices. *IEEE Access*, 3: 89-98. doi: 10.1109/ACCESS.2015.2406292.
- [8] Hu AP, Liu C, Li HL. (2008) A novel contactless battery charging system for soccer playing robot. In 2008 15th International Conference on Mechatronics and Machine Vision in Practice (pp. 646-650). IEEE.
- [9] Kline M, Izyumin I, Boser B, Sanders S. (2011) Capacitive power transfer for contactless charging. In 2011 Twenty-Sixth Annual IEEE Applied Power Electronics Conference and Exposition (APEC) (pp. 1398-1404). IEEE.
- [10] Ludois DC, Reed JK, Hanson K. (2012) Capacitive power transfer for rotor field current in synchronous machines. *IEEE Transactions on Power Electronics*, 27(11): 4638-4645. doi: 10.1109/TPEL.2012.2191160.
- [11] Dai J, Ludois DC. (2015) Wireless electric vehicle charging via capacitive power transfer through a conformal bumper. In 2015 IEEE Applied Power Electronics Conference and Exposition (APEC) (pp. 3307-3313). IEEE.
- [12] Brown WC. (1984) The history of power transmission by radio waves. *IEEE Transactions on Microwave Theory and Techniques*, 32(9): 1230-1242. doi: 10.1109/TMTT.1984.1132833.
- [13] McSpadden JO, Mankins JC. (2002) Space solar power programs and microwave wireless power transmission technology. *IEEE Microwave Magazine*, 3(4): 46-57. doi: 10.1109/MMW.2002.1145675.
- [14] Karalis A, Joannopoulos JD, Soljačić M. (2008) Efficient wireless non-radiative mid-range energy transfer. *Annals of Physics*, 323(1):34-48. <https://doi.org/10.1016/j.aop.2007.04.017>
- [15] Raible DE, Dinca D, Nayfeh TH. (2011). Optical frequency optimization of a high intensity laser power beaming system utilizing VMJ photovoltaic cells. In 2011 International Conference on Space Optical Systems and Applications (ICSOS) (pp. 232-238). IEEE.
- [16] Cai M, Vahala K. (2000) Highly efficient optical power transfer to whispering-gallery modes by use of a symmetrical dual-coupling configuration. *Optics Letters*, 25(4): 260-262. <https://doi.org/10.1364/OL.25.000260>
- [17] Awal MR, Jusoh M, Sabapathy T, Kamarudin MR, Rahim RA. (2016) State-of-the-art developments of acoustic energy transfer. *International Journal of Antennas and Propagation*. <https://doi.org/10.1155/2016/3072528>
- [18] Awal MR, Jusoh M, Ahmad RB, Sabapathy T, Yasin MNM, Mat MH. (2019) Designing cantilever dimension for low power wireless applications. *Indonesian Journal Electrical Engineering and Computer Science*, 14(2): 758-764. <http://doi.org/10.11591/ijeecs.v14.i2.pp758-764>